IEEE Access
Multidisciplinary | Rapid Review | Open Access Journal

Received May 21, 2020, accepted May 27, 2020, date of publication May 29, 2020, date of current version June 12, 2020.

Digital Object Identifier 10.1109/ACCESS.2020.2998698

Adaptive Fractional-Order SMC Controller Design for Unmanned Quadrotor Helicopter Under Actuator Fault and Disturbances

XIAOYU SHI[1], YUHUA CHENG[1], (Senior Member, IEEE), CHUN YIN[1], (Member, IEEE), SHOUMING ZHONG[2], XUEGANG HUANG[3], KAI CHEN[1], AND GEN QIU[1]

[1]School of Automation Engineering, University of Electronic Science and Technology of China, Chengdu 611731, China
[2]School of Mathematics Science, University of Electronic Science and Technology of China, Chengdu 611731, China
[3]Hypervelocity Aerodynamics Institute, China Aerodynamics Research and Development Center, Mianyang 621000, China

Corresponding author: Yuhua Cheng (yhcheng@uestc.edu.cn)

This work was supported in part by the National Basic Research Program of China under Grant 61873305 and Grant U1830207, in part by the Sichuan Science and Technology Plan Project under Grant 2018JY0410 and Grant 2019YJ0199, and in part by the Grant 19kfek04.

ABSTRACT This paper presented an adaptive and fractional-order sliding mode control(FOSMC) method for the unmanned quadrotor helicopter. The aircraft system includes actuator fault and external disturbances. The switching sliding mode law enables the system to reach the predefined sliding surface from arbitrary states. Then the equation control law keeps the trajectory stay over the sliding hyperplane. In order to make sure sliding motion from the arbitrary states to the surface within limited time, a novel fractional-order power switching control law is developed. System actuator failures are compensated online with adaptive control laws. The controllers are derived from the Lyapunov theory, which guarantees that the controllability and feasibility. This novel control strategy has higher tracking accuracy through the timely faults and disturbances compensation law. The presented fractional-order sliding mode scheme improves the speed of system convergence and shortens the reaching time. The adaptive strategy estimated the bounds of the disturbances and good robustness has been achieved. Simulation results shown that the presented strategy has numerous advantages in terms of attitude and position tracking.

INDEX TERMS Fractional-order switching-type control law, adaptive sliding mode technique, unmanned quadrotor helicopter.

I. INTRODUCTION

In the last few decades, academic research and engineering applications on unmanned quadrotor helicopters has attracted more and more scholars' attention. Unmanned quadrotor helicopters have unique advantages such as: vertical taking off and landing with taxiway, broad Flight mode ranges from hovering to cruising, good mobility in restricted environments [1]–[5]. Therefore, the UAVs has been widely used in military and civil fields which include attacks and defenses, disaster relief, space surveillance, supervision, and so on [6]–[8].

The unmanned quadrotor helicopters are a category of relatively simple aircraft system, which attract scholars pay close attention to research. The industrial and academic territories are interesting and necessary among the various kind of helicopters. Nevertheless, it is a nonlinear strongly coupled dynamic system. Therefore, it is still a complex and difficult problem to design robust controllers of unmanned quadrotor helicopters [9]–[11]. At present, the scholars have obtained a series of valuable results about the robust stability controller design of the unmanned quadrotor helicopter. A variety of intelligent and advanced and valid control methodologies have been developed, such as PID control, adaptive law control, neural network control (NN), model predictive control (MPC), backstepping, et al [12]–[19]. Boubertakh et al combined the traditional PID method with fuzzy control to design controllers for the stable of a quadrotor [12]. Nonlinear model predictive control (MPC) has been developed for a kind of small scale of quadrotor [15]. For nonlinear large-scale systems, Du et al presented a adaptive finite time method combined with backstepping approach [16]. Dalamagkidis et al demonstrated the model predictive control and neural network strategy for a kind of unmanned helicopters [18].

The associate editor coordinating the review of this manuscript and approving it for publication was Shihong Ding.

Das et al designed a backstepping controllers for the quadrotors [19]. The Lyapunov method provides a theoretical basis for the stability of the above methods [20], [21]. However, in the above mentioned research, the robustness and stability of the system need to be further improved, especially consider the disturbances and faults in the system.

Nevertheless, sliding mode control scheme got more attention because of the numerous advantages compared with other control method. It's robust to the parameter uncertainties and disturbances of the dynamic system. In addition, it is unsensitive to the system states variation and has been widely used in automated system especially for the quadrotors [22]–[25]. Chen et al presented the adaptive global sliding mode control (SMC) for the helicopter which includes the input time delay [26]. The feedback linearization (FL) and sliding mode control (SMC) algorithm have been discussed for the nonlinear helicopter [27]. The backstepping sliding-mode control (BSMC) [28] has been illustrated for the quadrotor.

However, these traditional sliding mode control methods do not guarantee that the system reaches the sliding surface in a limited time. Meanwhile, fractional-order (FO) controllers have been widely demonstrated that it has faster convergence and better stability than their IO counterparts. Thus, FO controllers have been broadly applied for complex systems, such as robot manipulators, helicopter, fractional chaotic system, [29]–[31].

Furthermore, the safety and reliability of the unmanned quadrotor helicopter is worth considering because of the complex and constrained flight environment. On the one hand, the structural characteristics of the unmanned quadrotor helicopter make it easy to have unknown parameters and disturbances of the model. And it is important to ensure that the system converges in a limited time and has good robustness [32]–[36]. On the other hand, it is unavoidable that the actuator failures after long-term service processes. Many fault detection and diagnosis (FDD) algorithms have been developed which regarded as a monitoring system by detecting, orientating, and identifying faults after the fault occur [37], [38]. FDD is a hysteresis system that does not allow real-time adjustment of system failures. So, it is not adequate to ensure the system safe operation. They are significant feature that are capable of maintaining the good performance in the presence of actuator failures. The fault-tolerant control (FTC) algorithms are capable of ensuring that the system still maintain a certain performance subject to faulty conditions [39]–[41]. Geng et al designed the FTC used on the sensors based on Kalman filter method [40].

For a kind of flexible spacecraft [41], a robust FTC has been demonstrated against actuator faults. But many of the current control methods treat disturbances and faults as a bounded signal. This will degrade the system performance.Fractional sliding mode control algorithm can improve the robust performance of the system.The effective FO-sliding mode controller have been utilized in various systems [42]–[44].Pashaei et al constructed a disturbance observer for a kind of dynamic systems [45]. For the position servo system, the FO-SMC are used to compensate the uncertainties and fault [46]. Adaptive sliding mode control and backstepping fast terminal sliding mode has been discussed for Mofid and Labbadi and Cherkaoui [47] and Mofid and Mobayen [48]. Based on the above analysis, it is an important topic to be researched.

In order to figure out the aforementioned problems, this article proposes a fractional-order adaptive sliding mode control strategy to realize robust stability control of the unmanned helicopter system. The main contribution of this paper can be described as follows. 1.) The model of the quadrotor has been improved and the coupling between attitude and position was also calculated while considering the actuator failure and external disturbances. All state variables reach the sliding hyperplane at finite time and globally asymptotically converges to the equilibrium. 2.) Adaptive control law accelerates system convergence speed and ensures system stability through real-time compensation. 3.) Compared with the traditional sliding mode surface, the fractional sliding mode control law effectively reduce chattering, thereby improving the stability of the system. 4.) It improves the fault tolerance performance of the system while considering actuator failure. And the control law designed in this paper effectively resist the failures. The reminder of this research is organized as follows. Section II described the dynamic mode of the unmanned quadrotor helicopter and the physical parameters are given. Section III developed the detailed design process of the presented control methodology. The numerical simulation includes various trajectory are accessed in Section IV. Finally, the conclusions and future research work are summarized and presented in Section V.

II. PROBLEM DESCRIPTION AND PRELIMINARIES

The UAVs play a crucial role in both military and civilian applications. The rotor UAVs have received much attention due to their flexibility and low cost. The unmanned quadrotor helicopters are representative and have been broadly used in many applications, such as payload transportation, air quality monitoring, *et al.* The structure of the unmanned quadrotor helicopter researched in this paper is depicted in Fig. 1. It consists of four propellers in the cross configuration and which distributed on four axes of rotation parallelly and symmetrically.

The description of the unmanned quadrotor helicopter includes both position and attitude. The earth coordinate system and the body coordinate system are employed to describe the dynamic of the unmanned quadrotor helicopter. The origin of inertial frame uses a point on the ground to establish a right-handed system. The origin of the body frame is defined as the center of the unmanned quadrotor helicopter. The axes of the inertial frame are denoted as $(O_E\_X_E, Y_E, Z_E)$, while the another are denoted as $(O_B\_X_B, Y_B, Z_B)$. Secondly, the following related variables are defined, namely the position and angle based on the inertial coordinate system, $\xi^E = [x, y, z]^T$, $\vartheta^E = [\phi, \theta, \psi]^T$, and the velocity and

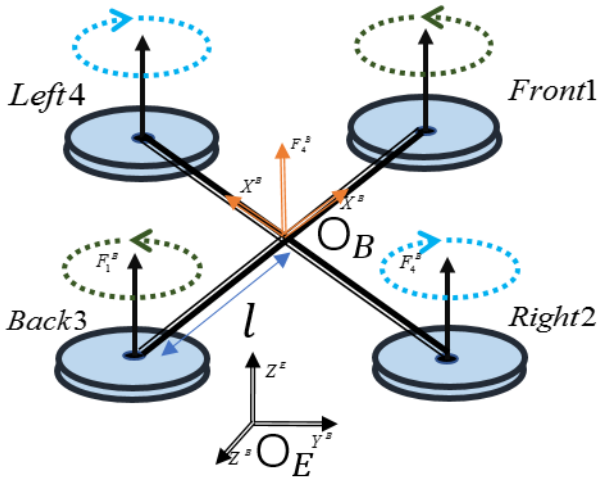

FIGURE 1. The configuration of the unmanned quadrotor helicopter.

angulars velocity based on the body coordinate system, $V^B = [u, v, w]^T$, $W^B = [p, q, r]^T$.

According to the structure of the unmanned quadrotor helicopter, the control of various flight attitudes and positions are achieved by adjusting the speed of the propellers. The basic movements of the quadrotor include hovering, vertical motion, rolling motion, pitching motion and yaw motion. When the rotation speeds of the four propellers are the same, the total lift is equal to the self-gravity of the system structure, so the system is in a hovering state. Similarly, when the total lift is not equal to its own gravity, it will take off and land vertically. The total lift around z axis is given as $U_z = \sum_{i=1}^{4} b\Omega_i^2$. The current rear rotor speed is the same and the left and right rotor speeds are different, a rolling motion through a moment about the x-axis is obtained. The moment along x axis is given as $U_\phi = bl(\Omega_4^2 - \Omega_2^2)$. In contrast, a pitch motion around the y-axis is generated and the moment is $U_\theta = bl(\Omega_3^2 - \Omega_1^2)$. The yaw motion is achieved by changing the rotational speed of the four rotors. The torsional moment is $U_\psi = \sum_{i=1}^{4} (-1)^i d\Omega_i^2$.

Therefore, the relationship between the control inputs of the actuator and the speed of the propellers can be described as:

$$\begin{bmatrix} U_z \\ U_\phi \\ U_\theta \\ U_\psi \end{bmatrix} = \begin{bmatrix} b & b & b & b \\ 0 & -bl & 0 & bl \\ -bl & 0 & bl & 0 \\ -d & d & -d & d \end{bmatrix} \begin{bmatrix} \Omega_1^2 \\ \Omega_2^2 \\ \Omega_3^2 \\ \Omega_4^2 \end{bmatrix} \tag{1}$$

where b is lift coefficient, l denotes the disturbance between the center of the unmanned quadrotor helicopter with the rotation propeller, $\Omega_i, i = 1, 2, 3, 4$ expresses the speed of the rotors.

The force and moment equalities of the unmanned quadrotor helicopter can be viewed as:

$$\begin{bmatrix} F^E \\ \Gamma^B \end{bmatrix} = \begin{bmatrix} m & 0 \\ 0 & I \end{bmatrix} \begin{bmatrix} \ddot{\xi}^E \\ \dot{W}^B \end{bmatrix} + \begin{bmatrix} 0 \\ W^{B^T} \times (IW^B) \end{bmatrix} \tag{2}$$

where $F^E = \begin{bmatrix} F_x & F_y & F_z \end{bmatrix}^T$ is the total forces based on the earth frame, $\Gamma^B = \begin{bmatrix} \Gamma_x & \Gamma_y & \Gamma_z \end{bmatrix}$ is the total moments through the body frame, $I = diag(I_x, I_y, I_z)$ indicates the diagonal inertial matrix of the quadrotor helicopter, m represents the mass of the quadrotor system.

Further, the forces on the aircraft which includes the lift, drag and gravity are given as:

$$\begin{aligned} F^E &= F_f + F_d + F_g \\ &= \begin{bmatrix} s\theta c\psi c\phi + s\psi s\phi \\ s\theta s\psi c\phi - c\psi s\phi \\ c\theta c\phi \end{bmatrix} b \sum_{i=1}^{4} \Omega_i^2 \\ &\quad + \begin{bmatrix} -K_{dx}\dot{x} \\ -K_{dy}\dot{y} \\ -K_{dz}\dot{z} \end{bmatrix} + \begin{bmatrix} 0 \\ 0 \\ -mg \end{bmatrix} \end{aligned} \tag{3}$$

where K_{dx}, K_{dy}, K_{dz} are drag coefficients, g is acceleration of gravity, $s(\cdot) \triangleq \sin(\cdot)$, $c(\cdot) \triangleq \cos(\cdot)$.

Meanwhile, the moments on the aircraft are shown as:

$$\begin{aligned} \Gamma^B &= \Gamma_f + \Gamma_a + \Gamma_g \\ &= \begin{bmatrix} lb(\Omega_4^2 - \Omega_2^2) \\ lb(\Omega_3^2 - \Omega_1^2) \\ \sum_{i=1}^{4} (-1)^i d\Omega_i^2 \end{bmatrix} + \begin{bmatrix} -K_{ax}\dot{\phi}^2 \\ -K_{ay}\dot{\theta}^2 \\ -K_{az}\dot{\psi}^2 \end{bmatrix} \\ &\quad + \begin{bmatrix} -I_r q \sum_{i=1}^{4} (-1)^i \Omega_i \\ I_r p \sum_{i=1}^{4} (-1)^i \Omega_i \\ 0 \end{bmatrix} \end{aligned} \tag{4}$$

where K_{ax}, K_{ay}, K_{az} are aerodynamics friction coefficients, I_r is the inertial moment of the quadrotor propeller.

The relationship between the Euler angle rates and angular velocities are:

$$\begin{bmatrix} \dot{\phi} \\ \dot{\theta} \\ \dot{\psi} \end{bmatrix} = R \begin{bmatrix} p \\ q \\ r \end{bmatrix}, R = \begin{bmatrix} 1 & s\phi t\theta & c\phi t\theta \\ 0 & c\phi & -s\phi \\ 0 & s\phi \sec\theta & c\phi \sec\theta \end{bmatrix} \tag{5}$$

Assumption 2.1: The changes of the roll and pitch angles are very small, so the following equations can be got $\sin\phi \approx 0$, $\sin\theta \approx 0$, $\cos\phi \approx 1$, $\cos\theta \approx 1$.

Therefore, the matrix can be simplifies as identity matrix, i.e $\begin{bmatrix} \dot{\phi} & \dot{\theta} & \dot{\psi} \end{bmatrix}^T = \begin{bmatrix} p & q & r \end{bmatrix}^T$.

Substitute the Eq.(3)(4) into Eq.(2), the transactional and rotational dynamic model can be expressed as:

$$\begin{aligned} m \begin{bmatrix} \ddot{x} \\ \ddot{y} \\ \ddot{z} \end{bmatrix} &= \begin{bmatrix} s\theta c\psi c\phi + s\psi s\phi \\ s\theta s\psi c\phi - c\psi s\phi \\ c\theta c\phi \end{bmatrix} b \sum_{i=1}^{4} \Omega_i^2 \\ &\quad + \begin{bmatrix} -K_{dx}\dot{x} \\ -K_{dy}\dot{y} \\ -K_{dz}\dot{z} \end{bmatrix} + \begin{bmatrix} 0 \\ 0 \\ -mg \end{bmatrix} \end{aligned} \tag{6}$$

$$\begin{bmatrix} I_x\ddot{\phi}+\dot{\theta}\dot{\psi}(I_z-I_y) \\ I_y\ddot{\theta}+\dot{\phi}\dot{\psi}(I_x-I_z) \\ I_z\ddot{\psi}+\dot{\phi}\dot{\theta}(I_y-I_x) \end{bmatrix} = \begin{bmatrix} lb(\Omega_4^2-\Omega_2^2) \\ lb(\Omega_3^2-\Omega_1^2) \\ \sum_{i=1}^{4}(-1)^i d\Omega_i^2 \end{bmatrix} + \begin{bmatrix} -K_{ax}\dot{\phi}^2 \\ -K_{ay}\dot{\theta}^2 \\ -K_{az}\dot{\psi}^2 \end{bmatrix} + \begin{bmatrix} -I_r q\sum_{i=1}^{4}(-1)^i\Omega_i \\ I_r p\sum_{i=1}^{4}(-1)^i\Omega_i \\ 0 \end{bmatrix} \tag{7}$$

The faults of the quadrotor UAV actuators generally include the following categories through the performance of the fault [49].

Firstly, we assume that $u_d(t)$ is the expected value generated by the control module and $u_a(t)$ is the actual output of the actuator. When the actuator does not malfunction, the actual control should be consistent with the desired control information, that is, $u_d(t) = u_a(t)$. When the actuator is in the fault state, the actual output control of the system will deviate from the desired control information. If the four actuators of the quadrotor UAV are described as i, $i = 1, 2, 3, 4$, then the fault model can be recorded as:

$$u_{ai}(t) = \rho_i(t)u_{di}(t) + d_i(t), \quad \forall t \geq T_i. \tag{8}$$

where $\rho_i(t) \in [0, 1]$. And $\forall t < T_i$ the states of the system are normal.

(1.) Bias fault of actuator: a kind of typical additive faults, $\rho_i(t) = 1, d_i(t) \neq 0$. The actual torque of the actuator has a bias compared to the desired torque, which is independent of time. The mathematical model of the fault is $u_{ai}(t) = \rho_i(t)u_{di}(t) + d_i, \forall t \geq T_i$.

(2.) Drift fault of actuator: a class of additive faults, $\rho_i(t) = 1, d_i(t) \neq 0$. Similar to the actuator bias fault, the only difference is that the actual output torque is time dependent, i.e. $u_{ai}(t) = \rho_i(t)u_{di}(t) + d_i(t), \forall t \geq T_i$.

(3.) Loss of effectiveness of actuator: a category of multiplicative faults, $\rho_i(t) \neq 0, d_i(t) = 0$. The actual torque of the actuator is proportionally reduced compared to the desired control torque, i.e. the actuator loses some of its execution effectiveness. Its mathematical model can be expressed as $u_{ai}(t) = \rho_i(t)u_{di}(t), \forall t \geq T_i$.

In addition, quadrotor UAVs need to carry out missions in different complex environments that the human can accomplish. The complex and variable environment brings greater challenges to the research of quadrotor UAVs. It is also conceivable that the changing environment can cause flight difficulties. We classify these as uncertain external disturbances. At present, a large number of scholars describe perturbations as stationary constant perturbations and random perturbations.

$$\begin{cases} \ddot{x} = (s\theta c\phi c\psi + s\phi s\psi)\dfrac{U_z+f_1(t)}{m} - \dfrac{K_{dx}\dot{x}}{m} + d_x, \\ \ddot{y} = (s\theta c\phi s\psi - s\phi c\psi)\dfrac{U_z+f_1(t)}{m} - \dfrac{K_{dy}\dot{y}}{m} + d_y, \\ \ddot{z} = (c\theta c\phi)\dfrac{U_z+f_1(t)}{m} - g - \dfrac{K_{dz}\dot{z}}{m} + d_z, \end{cases} \tag{9}$$

TABLE 1. Parameter values for the quadrotor UAV.

m	$0.53kg$
g	$9.81\ m/s^2$
d	$7.5 \times 10^{\wedge(-7)}$
b	$3.13 \times 10^{\wedge(-5)}$
l	$0.232m$
$I = diag(I_x, I_y, I_z)$	$0.00628kg \cdot m^2$
I_r	$0.002kg \cdot m^2$
K_{dx}, K_{dy}	$5.567 \times 10^{\wedge(-4)}$
K_{ax}, K_{ay}	$5.567 \times 10^{\wedge(-4)}$
K_{dz}	$6.345 \times 10^{\wedge(-4)}$
K_{az}	$6.345 \times 10^{\wedge(-4)}$

$$\begin{cases} \ddot{\phi} = \dfrac{I_y-I_z}{I_x}\dot{\theta}\dot{\psi} - \dfrac{K_{ax}\dot{\phi}^2}{I_x} - \dfrac{I_r}{I_x}\Omega\dot{\theta} + \dfrac{U_\phi+f_2(t)}{I_x} + d_\phi, \\ \ddot{\theta} = \dfrac{I_z-I_x}{I_y}\dot{\phi}\dot{\psi} - \dfrac{K_{ay}\dot{\theta}^2}{I_y} + \dfrac{I_r}{I_y}\Omega\dot{\phi} + \dfrac{U_\theta+f_2(t)}{I_y} + d_\theta, \\ \ddot{\psi} = \dfrac{I_x-I_y}{I_z}\dot{\phi}\dot{\theta} - \dfrac{K_{az}\dot{\psi}^2}{I_z} + \dfrac{U_\psi+f_2(t)}{I_z} + d_\psi. \end{cases} \tag{10}$$

where $f_i(t)$, $i = 1, 2, 3, 4$ represents the fault of the actuators. $d_\xi = \begin{bmatrix} d_x & d_y & d_z \end{bmatrix}^T$, $d_\vartheta = \begin{bmatrix} d_\phi & d_\theta & d_\psi \end{bmatrix}^T$ are the external disturbances include sudden and unexpected wind fields. The physics parameters of the unmanned quadrotor helicopter are shown as Table 1.

III. ADAPTIVE FRACTIONAL ORDER SMC CONTROLLER DESIGN AND STABILITY ANALYSIS

In this section, an adaptive fractional power sliding mode controller has been established. On the one hand, it ensures that the system reach the steady state in a limited time, on the other hand, the adaptive control law and switching sliding mode law have been designed to compensate for actuator failures and external disturbances which contained in the system. The fractional power-switching control law effectively reduce the system chattering, and also make the system reaches the equilibrium point at limited time. The sliding mode power switching law can speed up the system convergence speed. This allows the system converge to a balanced state quickly and accurately. The adaptive control law designed for actuator failure does not require advance prediction of the fault and enables online adjustment of the fault. The structure of the method studied in this paper is shown in Fig. 2.

A. FINITE-TIME FRACTIONAL-ORDER SMC CONTROLLER DESIGN

In this section, a valuable controller has been established so that the actual flight state of the unmanned quadrotor helicopter tracking the reference signal well. It is seen that the attitude system is decoupled from the dynamic model and is fully actuated. However, the position system is underactuated and it is controlled by the thrust force. The desired reference trajectory of the unmanned quadrotor helicopter is defined as $R=\begin{bmatrix} z_r & \phi_r & \theta_r & \psi_r \end{bmatrix}^T$, and the actual output trajectory is $A = \begin{bmatrix} z & \phi & \theta & \psi \end{bmatrix}^T$. The controller designed in this paper

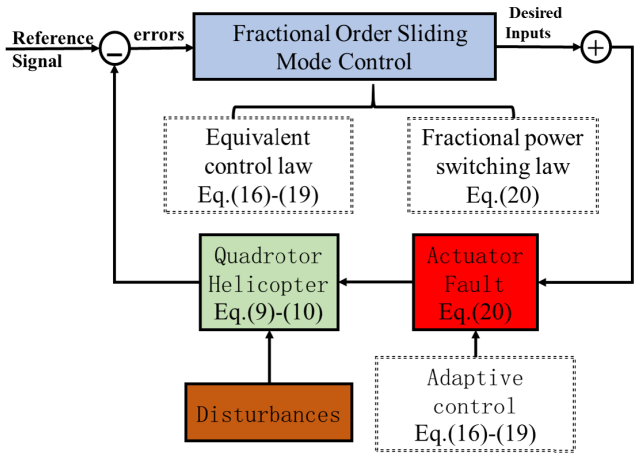

FIGURE 2. The structure of the proposed FO-FTC for the quadrotor.

guarantee that the system state variable error converges to 0. At first, the tracking errors can be defined as: $e_{z1} = z - z_r$, $e_{\phi 1} = \phi - \phi_r, e_{\theta 1} = \theta - \theta_r, e_{\psi 1} = \psi - \psi_r, e_{z2} = \dot{e}_{z1} + c_1 e_{z1}, e_{\phi 2} = \dot{e}_{\phi 1} + c_1 e_{\phi 1}, e_{\theta 2} = \dot{e}_{\theta 1} + c_1 e_{\theta 1}, e_{\psi 2} = \dot{e}_{\psi 1} + c_1 e_{\psi 1}$, where c_1, c_2, c_3, c_4 are non-zero positive parameters.

An effectiveness sliding surface is employed to constructed the controller.With the tracking errors, the sliding manifolds can be given as:

$$\begin{cases} s_z = e_{z2} + k_1 e_{z1}, \\ s_\phi = e_{\phi 2} + k_2 e_{\phi 1}, \\ s_\theta = e_{\theta 2} + k_3 e_{\theta 1}, \\ s_\psi = e_{\psi 2} + k_4 e_{\psi 1}, \end{cases} \tag{11}$$

where k_1, k_2, k_3, k_4 are non-zero positive parameters.

Based on $\dot{s}_A(t) = 0, A = \begin{bmatrix} z & \phi & \theta & \psi \end{bmatrix}$, the equivalent control law of the system can be obtained, which ensures that the system reaches the equilibrium point.

$$\dot{s}_z(t) = \dot{e}_{z2} + k_1 \dot{e}_{z1} = (\cos\theta \cos\phi)\frac{U_1}{m} - g - \frac{K_{dz}\dot{z}}{m} - \ddot{z}_r + (c_1 + k_1)\dot{e}_{z1}. \tag{12}$$

$$\dot{s}_\phi(t) = \dot{e}_{\phi 2} + k_2 \dot{e}_{\phi 1} = \frac{I_y - I_z}{I_x}\dot{\theta}\dot{\psi} - \frac{K_{ax}\dot{\phi}^2}{I_x} - \frac{I_r}{I_x}\Omega\dot{\theta} + \frac{U_2}{I_x} - \ddot{\phi}_r + (c_2 + k_2)\dot{e}_{\phi 1}. \tag{13}$$

$$\dot{s}_\theta(t) = \dot{e}_{\theta 2} + k_3 \dot{e}_{\theta 1} = \frac{I_z - I_x}{I_y}\dot{\phi}\dot{\psi} - \frac{K_{ay}\dot{\theta}^2}{I_y} + \frac{I_r}{I_y}\Omega\dot{\phi} + \frac{U_3}{I_y} - \ddot{\theta}_r + (c_3 + k_3)\dot{e}_{\theta 1}. \tag{14}$$

$$\dot{s}_\psi(t) = \ddot{e}_{\psi 2} + k_4 \dot{e}_{\psi 1} = \frac{I_x - I_y}{I_z}\dot{\phi}\dot{\theta} - \frac{K_{az}\dot{\psi}^2}{I_z} + \frac{U_4}{I_z} - \ddot{\psi}_r + (c_4 + k_4)\dot{e}_{\psi 1}. \tag{15}$$

After designing the sliding surface, the equivalent control law can be demonstrated. Therefore, the four equivalent

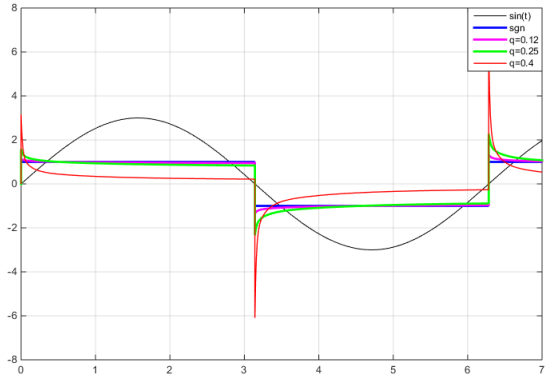

FIGURE 3. Comparison of different fo-smc.

control laws are viewed as

$$U_{1eq} = \frac{m}{\cos\theta\cos\phi}[g + \frac{K_{dz}\dot{z}}{m} + \ddot{z}_r - (c_1 + k_1)\dot{e}_{z1}]. \tag{16}$$

$$U_{2eq} = I_x[-\frac{I_y - I_z}{I_x}\dot{\theta}\dot{\psi} + \frac{K_{ax}\dot{\phi}^2}{I_x} + \frac{I_r}{I_x}\Omega\dot{\theta} + \ddot{\phi}_r - (c_2 + k_2)\dot{e}_{\phi 1}]. \tag{17}$$

$$U_{3eq} = I_y[-\frac{I_z - I_x}{I_y}\dot{\phi}\dot{\psi} + \frac{K_{ay}\dot{\theta}^2}{I_y} - \frac{I_r}{I_y}\Omega\dot{\phi} + \ddot{\theta}_r - (c_3 + k_3)\dot{e}_{\theta 1}]. \tag{18}$$

$$U_{4eq} = I_z[-\frac{I_x - I_y}{I_z}\dot{\phi}\dot{\theta} + \frac{K_{az}\dot{\psi}^2}{I_z} + \ddot{\psi}_r - (c_4 + k_4)\dot{e}_{\psi 1}]. \tag{19}$$

The Fractional order power switching control law is given as:

$$u_{sw} = \lambda_i |s_A|^{\alpha_i} D^{\beta_i}(sign(s_A)), \quad i = 1, 2, 3, 4. \tag{20}$$

Lemma 3.1: The Riemann-Liouville definition of the $\beta - th$ derivative is given as $D^\beta \zeta(t) = \frac{1}{\Gamma(n-\beta)}(\frac{d}{dt})^n \int_0^t \frac{\zeta(\tau)}{(t-\tau)^{1+\beta-n}} d\tau$, For $D^\beta \zeta(t) = \frac{1}{\Gamma(n-\beta)}(\frac{d}{dt})^n \int_0^t \frac{\zeta(\tau)}{(t-\tau)^{1+\beta-n}} d\tau$ and the fractional order satisfy $0 \le \beta < 1$, the following conclusion can be obtained, $D^\beta sign(\zeta(t)) \begin{cases} > 0, if\, \zeta(t) > 0 \\ < 0, if\, \zeta(t) > 0 \end{cases}$.

The important property of fractional sign has been proved [13]. In order to explain the characteristics of the fractional sign function, a sinusoidal signal $sin(t)$ has been selected as the original function. Fig.3 shows the graph of the function passing through the fractional sign function.

Remark 3.1: When the system switches the sliding mode control law, a larger amplitude can speed up the system response speed. So fractional sliding mode control reduces the time that for the system to reach equilibrium. Then it reaches to a value which is smaller than sgn function. It is helpful to reduce system chattering, thereby improving system stability and robustness.

So, combine the switching control law Eq.(24) with the equivalent controllers Eq.(16)-Eq.(19), the adaptive laws

Eq.(20)-Eq.(23), the controllers can be rearranged as:

$$U_1 = \frac{m}{\cos\theta\cos\phi}[g + \frac{K_{dz}\dot{z}}{m} + \ddot{z}_r - (c_1 + k_1)\dot{e}_{z1} - \lambda_1|s_z|^{\alpha_1}D^{\beta_1}(sign(s_z))]. \quad (21)$$

$$U_2 = I_x[-\frac{I_y - I_z}{I_x}\dot{\theta}\dot{\psi} + \frac{K_{d\phi}\dot{\phi}^2}{I_x} + \frac{I_r}{I_x}\Omega\dot{\theta} + \ddot{\phi}_r - (c_2 + k_2)\dot{e}_{\phi 1} - \lambda_2|s_\phi|^{\alpha_2}D^{\beta_2}(sign(s_\phi))]. \quad (22)$$

$$U_3 = I_y[-\frac{I_z - I_x}{I_y}\dot{\phi}\dot{\psi} + \frac{K_{d\theta}\dot{\theta}^2}{I_y} - \frac{I_r}{I_y}\Omega\dot{\phi} + \ddot{\theta}_r - (c_3 + k_3)\dot{e}_{\theta 1} - \lambda_3|s_\theta|^{\alpha_3}D^{\beta_3}(sign(s_\theta))]. \quad (23)$$

$$U_4 = I_z[-\frac{I_x - I_y}{I_z}\dot{\phi}\dot{\theta} + \frac{K_{d\psi}\dot{\psi}^2}{I_z} + \ddot{\psi}_r - (c_4 + k_4)\dot{e}_{\psi 1} - \lambda_4|s_\psi|^{\alpha_4}D^{\beta_4}(sign(s_\psi))]. \quad (24)$$

Theorem 3.1: Consider the nonlinear strong coupled system Eq.(9), Eq.(10) with external disturbances, given the sliding hyperplane Eq.(11), by employing the controllers Eq.(21)-Eq.(24) the sliding motion can be achieved and the tracking errors converge to zero at limited time regardless of the external disturbances.

B. STABILITY ANALYSIS

Select the Lyapunov function as

$$V_A = \frac{1}{2}{s_A}^2(t). \quad (25)$$

Its time derivative is shown as:

$$\dot{V}_A = s_A(t)\dot{s}_A(t). \quad (26)$$

According to the above analysis, based on the Eq.(20), thus we can get the following condition,

$$s_A(t)\dot{s}_A(t) = -\lambda_i s_A(t)|s_A|^{\alpha_i}D^{\beta_i}(sign(s_A)). \quad (27)$$

Now, consider the following two cases, a.) When $s_A(0) > 0$, $\dot{s}_A(t) = -\lambda {s_A}^{\alpha_i}D^{\beta_i}(sign(s_A))$ hence, it is obtained that

$$\dot{s}_A(t){s_A}^{-\alpha_i} = -\lambda D^{\beta_i}(sign(s_A)). \quad (28)$$

The time integral of Eq.(28) is $\int_0^t \frac{\dot{s}_A(t)}{{s_A}^{\alpha_i}(t)} = \frac{s_A(t)-s_A(0)}{(1-\alpha){s_A}^{\alpha_i}(t)} = \frac{1}{1-\alpha_i}[{s_A}^{1-\alpha_i}(t) - {s_A}^{1-\alpha_i}(0)]$, $\int_0^t -\lambda D^{\beta_i}(sign(s_A)) = \frac{-\lambda t^{1-\beta_i}}{(1-\beta_i)\Gamma(1-\beta_i)}$.

Since $s_{(t_{reach})} = 0$ at $t = t_{reach}$, one has

$$t_{reach} = (\frac{{s_A}^{1-\alpha_i}(0)(1-\beta_i)\Gamma(1-\beta_i)}{\lambda(1-\alpha_i)})^{\frac{1}{1-\beta_i}}. \quad (29)$$

b.) When $s_A(0) < 0$, $\dot{s}_A(t) = -\lambda(-s_A)^{\alpha_i}D^{\beta_i}(sign(s_A))$ so,

$$\dot{s}_A(t)(-s_A)^{-\alpha_i} = -\lambda D^{\beta_i}(sign(s_A)). \quad (30)$$

thus the Eq.(30) can be obtained as $(-s_A(t))^{1-\alpha_i} - (-s_A(0))^{1-\alpha_i} = \frac{-\lambda_i(1-\alpha_i)t^{1-\beta_i}}{(1-\beta_i)\Gamma(1-\beta_i)}$.

Furthermore, when $t = t_{reach}$ the system reaches a steady state, and the solution is

$$t_{reach} = (\frac{(-s_A(0)^{1-\alpha_i})(1-\beta_i)\Gamma(1-\beta_i)}{\lambda_i(1-\alpha_i)})^{\frac{1}{1-\beta_i}}. \quad (31)$$

According to a)and b), the reaching time can be given that

$$t_{reach} = (\frac{|s_A(0)^{1-\alpha_i}|(1-\beta_i)\Gamma(1-\beta_i)}{\lambda_i(1-\alpha_i)})^{\frac{1}{1-\beta_i}}. \quad (32)$$

Remark 3.2: Fractional sliding mold surface not only retains the characteristics of general sliding mold surface, but also can better adjust the performance of the control system. In addition, based on Eq.(28)-Eq.(32), the relationship between the sliding mode surface coefficient and the stability time of the system is analyzed. It ensures that the system guarantees stable at a limited time.

Theorem 3.2: Consider the nonlinear strong coupled system Eq.(9), Eq.(10) with external disturbances and actuator faults, the sliding hyperplane Eq.(11) is effective. The Eq.(32) makes sure that the system asymptotic stability and achieved the tracking errors converge to zero regardless of the actuator faults and external disturbances at limited time.

According to Lyapunov's theory, the asymptotically stability is satisfied, and therefore, the system valued can reach a steady state. The pitch angle and yaw angle subsystem controller can also be demonstrated as the same way.

C. FAULT TOLERANT CONTROLLER AND STABILITY ANALYSIS

In order to establish a controller that can compensate for external disturbances and actuator failures, we establish the following adaptive control law.

$$\dot{\hat{f}}_1(t) = l_{11}s_z(t)\cos\phi\cos\theta, \quad \dot{\hat{d}}_z(t) = l_{12}s_z(t). \quad (33)$$

$$\dot{\hat{f}}_2(t) = \frac{1}{I_x}l_{21}s_\phi(t), \quad \dot{\hat{d}}_\phi(t) = l_{22}s_\phi(t). \quad (34)$$

$$\dot{\hat{f}}_3(t) = \frac{1}{I_y}l_{31}s_\theta(t), \quad \dot{\hat{d}}_\theta(t) = l_{32}s_\theta(t). \quad (35)$$

$$\dot{\hat{f}}_4(t) = \frac{1}{I_z}l_{41}s_\psi(t), \quad \dot{\hat{d}}_\psi(t) = l_{42}s_\psi(t). \quad (36)$$

where $l_{1i}, l_{2i}, i = 1, 2, 3, 4$ are non-zero positive parameters.

Remark 3.3: The disturbances d_ξ, d_ϑ can includes the external disturbances such as wind field and uncertain parameters which is unknown the bounds. Besides, the reference position and attitude trajectory are required to be a twice continuously differentiable vector function of time.

With the consideration of external disturbances and actuator faults of the unmanned quadrotor helicopter, the asymptotically stability condition will be analyzed and proved. The altitude subsystem is controlled by U_1 and the attitude subsystem is controlled by U_2, U_3, U_4. Therefore, the analysis includes two parts; the altitude system and attitude system.

$$U_{1f} = \frac{m}{\cos\theta\cos\phi}[g + \frac{K_{dz}\dot{z}}{m} + \ddot{z}_r - (c_1 + k_1)\dot{e}_{z1} - \lambda_1|s_z|^{\alpha_1}D^{\beta_1}(sign(s_z)) - \hat{d}_z(t)] - \hat{f}_1(t). \quad (37)$$

$$U_{2f} = I_x[-\frac{I_y - I_z}{I_x}\dot{\theta}\dot{\psi} + \frac{K_{d\phi}\dot{\phi}^2}{I_x} + \frac{I_r}{I_x}\Omega\dot{\theta} + \ddot{\phi}_r - (c_2 + k_2)\dot{e}_{\phi 1} - \lambda_2|s_\phi|^{\alpha_2}D^{\beta_2}(sign(s_\phi)) - \hat{d}_\phi(t)] - \hat{f}_2(t). \quad (38)$$

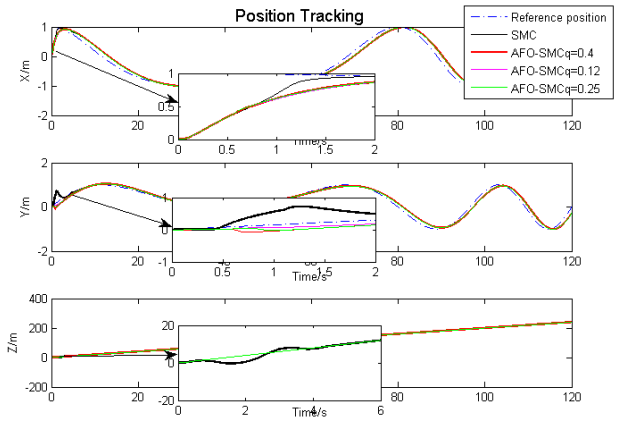

FIGURE 4. Position tracking performance in three directions.

$$U_{3f} = I_y[-\frac{I_z - I_x}{I_y}\dot{\phi}\dot{\psi} + \frac{K_{d\theta}\dot{\theta}^2}{I_y} - \frac{I_r}{I_y}\Omega\dot{\phi} + \ddot{\theta}_r - (c_3 + k_3)\dot{e}_{\theta 1} - \lambda_3|s_\theta|^{\alpha_3}D^{\beta_3}(sign(s_\theta)) - \hat{d}_\theta(t)] - \hat{f}_3(t). \tag{39}$$

$$U_{4f} = I_z[-\frac{I_x - I_y}{I_z}\dot{\phi}\dot{\theta} + \frac{K_{d\psi}\dot{\psi}^2}{I_z} + \ddot{\psi}_r - (c_4 + k_4)\dot{e}_{\psi 1} - \lambda_4|s_\psi|^{\alpha_4}D^{\beta_4}(sign(s_\psi)) - \hat{d}_\psi(t)] - \hat{f}_4(t). \tag{40}$$

Firstly, the candidate Lyapunov function for the altitude system can be employed as:

$$V_z = \frac{1}{2}{s_z}^2(t) + \frac{1}{2ml_{11}}\tilde{f}_1^2(t) + \frac{1}{2l_{12}}\tilde{d}_z^2(t). \tag{41}$$

Its time derivate is

$$\dot{V}_z = s_z(t)[(\cos\theta\cos\phi)\frac{U_1}{m} - g - \frac{K_{dz}\dot{z}}{m} - \ddot{z}_r + (c_1 + k_1)\dot{e}_{z1}] + \frac{1}{ml_{11}}\tilde{f}_1(t)(-\dot{\hat{f}}_1(t)) + \frac{1}{l_{12}}\tilde{d}_z(t)(-\dot{\hat{d}}_z(t)). \tag{42}$$

Substitute the control law Eq.(37) and adaptive law Eq.(33) into Eq.(42), the Eq.(42) can be rewritten as follows:

$$\begin{aligned}\dot{V}_z &= s_z(t)[d_z - \lambda_1|s_z|^{\alpha_1}D^{\beta_1}(sign(s_z)) - \hat{d}_z(t)] \\ &\quad + \tilde{f}_1(t)[\frac{s_z(t)(\cos\theta\cos\phi)}{m} - \frac{1}{ml_{11}}\dot{\hat{f}}_1(t)] \\ &\quad + \frac{1}{l_{12}}\tilde{d}_z(t)(-\dot{\hat{d}}_z(t)) \\ &= -\lambda_1 s_z(t)|s_z|^{\alpha_1}D^{\beta_1}(sign(s_z)) \\ &\quad + \tilde{f}_1(t)[\frac{s_z(t)(\cos\theta\cos\phi)}{m} - \frac{1}{ml_{11}}\dot{\hat{f}}_1(t)] \\ &\quad + \tilde{d}_z(s_z(t) - \frac{1}{l_{12}}\dot{\hat{d}}_z(t)) \\ &\le -\lambda_1 s_z(t)|s_z|^{\alpha_1}D^{\beta_1}(sign(s_z)) \\ &\le 0.\end{aligned} \tag{43}$$

According to theorem 3.1. and lemma 3.1., it can be obtained that $V_z > 0, \dot{V}_z \le 0$. Therefore, the inequality Eq.(43) concludes that the quadrotor position subsystem

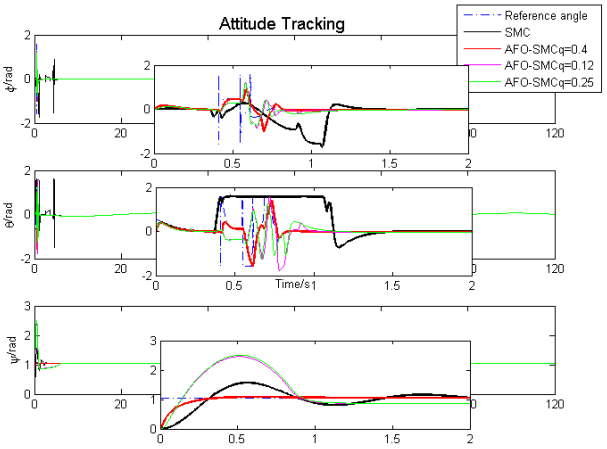

FIGURE 5. Attitude tracking performance in three directions.

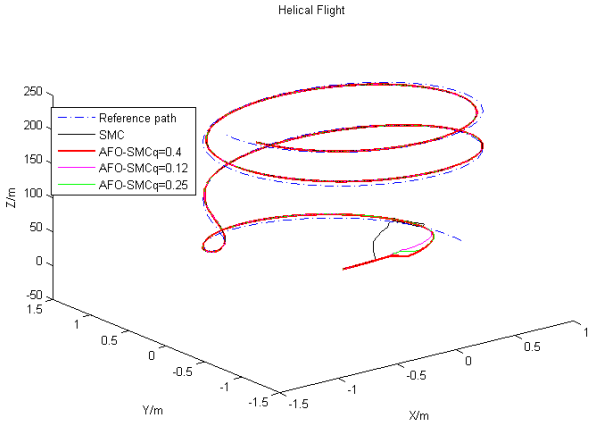

FIGURE 6. Trajectory tracking.

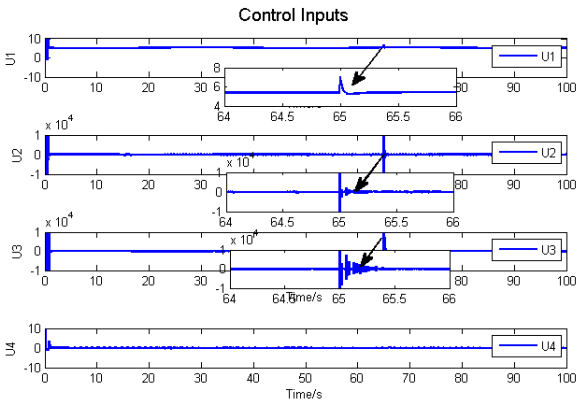

FIGURE 7. The control inputs of the quadrotor UAV.

Eq.(9) under the sliding mode controller Eq.(37) and adaptive law Eq.(33) is globally asymptotically stable.

Then the Lyapunov function of the rolling attitude subsystem is

$$V_\phi = \frac{1}{2}{s_\phi}^2(t) + \frac{1}{2l_{21}}\tilde{f}_2^2(t) + \frac{1}{2l_{22}}\tilde{d}_\phi^2(t). \tag{44}$$

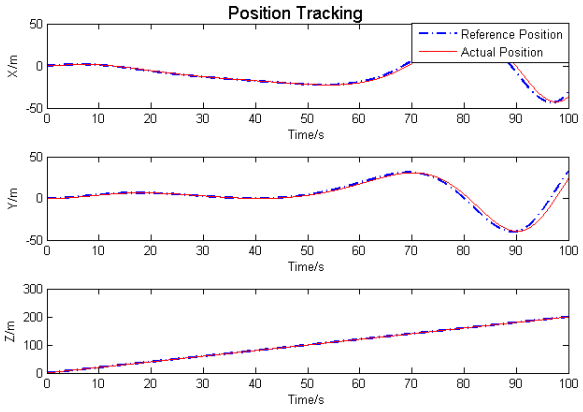

FIGURE 8. Position tracking performance in three directions.

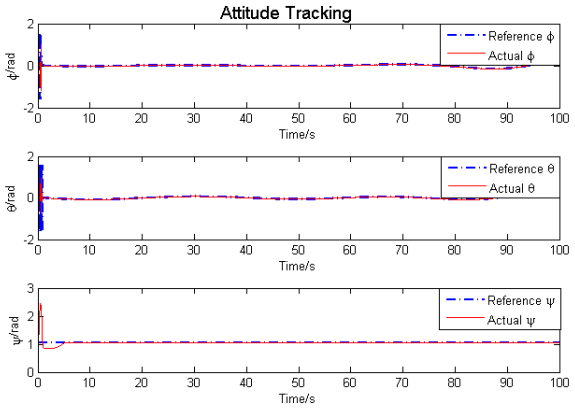

FIGURE 9. Attitude tracking performance in three directions.

Taking the derivative of Eq.(44), one has

$$\begin{aligned}\dot{V}_\phi &= s_\phi(t)[\frac{I_y - I_z}{I_x}\dot{\theta}\dot{\psi} - \frac{K_{d\phi}\dot{\phi}^2}{I_x} - \frac{I_r}{I_x}\Omega\dot{\theta} \\ &\quad + \frac{U_2 + f_2(t)}{I_x} + d_\phi(t) - \ddot{\phi}_r + c_2\dot{e}_\phi] \\ &\quad - \frac{1}{l_{21}}\tilde{f}_2(t)\dot{\hat{f}}_2(t) - \frac{1}{l_{22}}\tilde{d}_\phi(t)\dot{\hat{d}}_\phi(t). \end{aligned} \tag{45}$$

Adding the controller Eq.(38) and adaptive law Eq.(35) into the right side of Eq.(45), it concludes that

$$\begin{aligned}\dot{V}_\phi &= s_\phi(t)[d_\phi(t) - \lambda_2|s_\phi|^{\alpha_2}D^{\beta_2}(sign(s_\phi)) - \hat{d}_\phi(t)] \\ &\quad + \tilde{f}_\phi(t)[\frac{s_\phi(t)}{I_x} - \frac{1}{l_{21}}\dot{\hat{f}}_\phi(t)] - \frac{1}{l_{22}}\tilde{d}_\phi(t)\dot{\hat{d}}_\phi(t) \\ &\le -\lambda_2 s_\phi(t)|s_\phi|^{\alpha_2}D^{\beta_2}(sign(s_\phi)) \\ &\le 0. \end{aligned} \tag{46}$$

Theorem 3.3: Consider the nonlinear strong coupled system Eq.(9),Eq.(10) with external disturbances, actuator faults, given the sliding hyperplane Eq.(11), by employing the adaptive laws Eq.(33)-Eq.(36) and the controllers Eq.(37)-Eq.(40) the sliding motion can be achieved and the tracking errors converge to zero regardless of the actuator faults and external disturbances.

According to Lyapunov's theory, the asymptotically stability is satisfied, and therefore, the system valued can reach a steady state. The pitch angle and yaw angle subsystem controller can also be demonstrated as the same way.

IV. NUMERICAL EXAMPLES

In this section, the robustness and effectiveness of the proposed control strategy has been demonstrated. A series of numerical MTLAB tests based on the unmanned quadrotor helicopter systems are achieved. The performance of the position and attitude tracking problem have been verified. In addition, the aerodynamic forces and air drag are taken into consideration, which simulate a real helicopter. The controller parameters of the FO-sliding mode control scheme are shown $c_1 = 25, c_2 = 2.5, c_3 = 12, c_4 = 14$; $k_1 = 2$, $k_2 = 80, k_3 = 80, k_4 = 0.5$; $\lambda_i = 0.002, \alpha_i = 0.5$, $\beta_i = 0.4, i = 1, 2, 3, 4$.

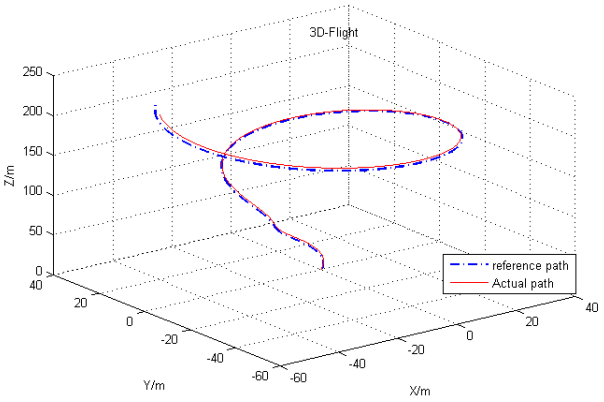

FIGURE 10. Trajectory tracking.

A. EXAMPLE 1

In the simulation results, the initial values of positions and angles for the studied unmanned quadrotor helicopter are zeros.

At first, we verify the performance of the controllers without fractional order power switching control law [47], [48]. The reference trajectory is shown as: $\left[x = \cos(\pi/40 * \tau);\ y = \sin(\pi/40 * \tau);\ z = 2 * t;\right], \tau = -0.025t^2 + 2t$. Fig.4 illustrated the position tracking. It's shown that there are larger chattering for the three directions at the first 5 seconds for the black line which represents the traditional sliding mode controller. For the other line, it's shown that the position control strategy can accuracy track the desired values within a short time. When $q = 0.4$, the FO-sliding mode controller has the best robustness. It's observed that the attitudes return to the desired values a long time as present Fig.5 for the sliding mode control method. The three attitudes converge to balance point with a short time through the presented strategy. As described in Fig.3, the fractional derivative of the sign function has the same positive and negative sign compared with the original function. It can be used as switching control scheme to make the system state approach to the sliding surface. The value of the fractional order sign function at the zero-crossing point is larger than the sign function. Then it's small than the

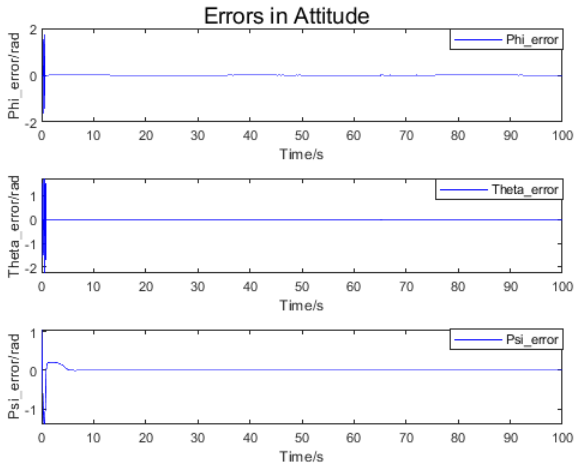

FIGURE 11. Attitude tracking error performance in three directions.

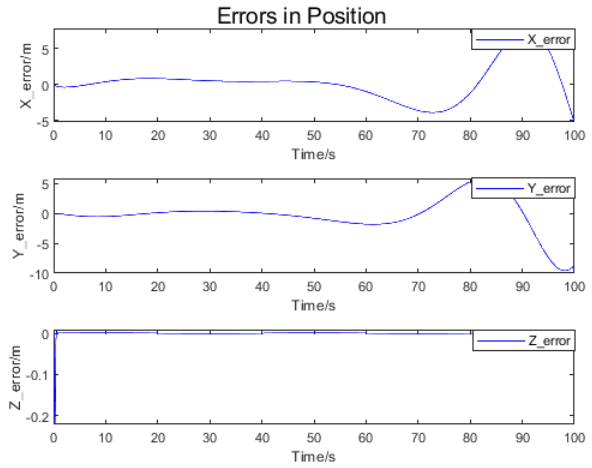

FIGURE 12. Position tracking error performance in three directions.

sign function. These characteristics make fractional sliding mode control law better than traditional sliding mode surfaces. The 3D trajectory tracking ability is displayed in Fig.6. According to this simulation,the traditional sliding mode controller is able to make the system reach equilibrium and stabilize. However, When the system reaches the equilibrium point, there is a large chatter, and it takes a long time to reach the equilibrium point.It is obvious that the actual trajectory tracking the reference signal very well for the red trajectory.

Compare the green line and red line in Figs. 4, positions in three directions converge stable point faster with less chattering based on the FO-SMC method. Similar, the attitude angles of the quadrotor in Figs. 5 are more stable than SMC method. Therefore, during the flight of a quadrotor UAV, the fractional sliding mode control method proposed in this paper would be more stable. The simulation results denotes that the robustness stability of the presented methodology against the external disturbances is better than the other methods.

B. EXAMPLE 2

This part is used for testing the stability of quadrotor system while encountering external disturbances and actuator fault. The perturbations are considered in the quadrotor model equations. The expression of disturbances are time-varying which caused by gusts of wind. In this simulation, the disturbance is represent as: $d = 0.5\sin(0.05\pi * t)$.

The control strategy described in Fig.7 managed to keep the attitude and position of the unmanned quadrotor helicopter to the stable states. As shown from Fig. 7, the actuator failure is existed in the first controller. However, it can be found that all the control inputs converge to the steady values in the presence of actuator faulty. Because the coupled characters of the unmanned quadrotor helicopter dynamic model, the controllers U_2, U_3 have been affected. However, all controllers converge to equilibrium states, it's also verifies the coupled characteristic of the system and the robust of the proposed methodology. Thus,the feasibility and robustness has been demonstrated again.

In addition, the disturbances are taken into consideration, so the effects of this part are invisible on all the state variables and four controllers. Then the applicability and robustness of the presented overall control strategy is demonstrated as shown in Figs.8 and 9. It is obvious that the attitude and position of the unmanned quadrotor helicopter model subject to external disturbances and actuator fault have good tracking performance. Finally, Fig. 10 exhibits the trajectory, so the presented tracking results are promising at the attitude and position tracking ability for the unmanned helicopter. And the errors are shown as Fig. 11 and Fig. 12. It is obvious the errors are small.

V. CONCLUSIONS

In this research, the position and attitude tracking problem of a class of unmanned helicopter has been studied based on the aforementioned control schemes. The advantages of the presented algorithm are verified through two examples. The primary contributions are shown as follows. Firstly, all states of the 6-DOF aircraft converge to desired signal respectively. Next, all state values reached the sliding hyperplane at limited time based on fractional order power switching control laws the and the chattering performance reduced as well. Then, the adaptive laws compensate the actuator fault online. Finally, numerical simulation has shown that the good tracking property of the depicted control methodology. In the future research, we will verify the effectiveness of the algorithm through flight tests and optimize the controller parameters. In addition, fault-tolerant control of actuators and sensors is also a part of the research.

REFERENCES

[1] A. Modirrousta and M. Khodabandeh, "A novel nonlinear hybrid controller design for an uncertain quadrotor with disturbances," *Aerosp. Sci. Technol.*, vol. 45, pp. 294–308, Sep. 2015.
[2] T. Jiang, D. Lin, and T. Song, "Finite-time backstepping control for quadrotors with disturbances and input constraints," *IEEE Access*, vol. 6, pp. 62037–62049, 2018.
[3] N. Wang, Q. Deng, G. Xie, and X. Pan, "Hybrid finite-time trajectory tracking control of a quadrotor," *ISA Trans.*, vol. 90, pp. 278–286, Jul. 2019.
[4] K. Eliker and W. Zhang, "Finite-time adaptive integral backstepping fast terminal sliding mode control application on quadrotor UAV," *Int. J. Control, Autom. Syst.*, vol. 18, no. 2, pp. 415–430, Feb. 2020.

[5] C. Yin, T. Xue, X. Huang, Y.-H. Cheng, S. Dadras, and S. Dadras, "Research on damages evaluation method with multi-objective feature extraction optimization scheme for M/OD impact risk assessment," *IEEE Access*, vol. 7, pp. 98530–98545, 2019.

[6] Y. M. Zhang, A. Chamseddine, C. A. Rabbath, B. W. Gordon, C.-Y. Su, S. Rakheja, C. Fulford, J. Apkarian, and P. Gosselin, "Development of advanced FDD and FTC techniques with application to an unmanned quadrotor helicopter testbed," *J. Franklin Inst.*, vol. 350, no. 9, pp. 2396–2422, Nov. 2013.

[7] A. Aswani, P. Bouffard, and C. Tomlin, "Extensions of learning-based model predictive control for real-time application to a quadrotor helicopter," in *Proc. Amer. Control Conf. (ACC)*, Jun. 2012, pp. 4661–4666.

[8] C. Yin, S. Dadras, X. Huang, Y. Chen, and S. Zhong, "Optimizing energy consumption for lighting control system via multivariate extremum seeking control with diminishing dither signal," *IEEE Trans. Autom. Sci. Eng.*, vol. 16, no. 4, pp. 1848–1859, Oct. 2019.

[9] H. Liu, Y. Yu, and Y. Zhong, "Robust trajectory tracking control for a laboratory helicopter," *Nonlinear Dyn.*, vol. 77, no. 3, pp. 621–634, Aug. 2014.

[10] R. Mebarki, V. Lippiello, and B. Siciliano, "Nonlinear visual control of unmanned aerial vehicles in GPS-denied environments," *IEEE Trans. Robot.*, vol. 31, no. 4, pp. 1004–1017, Aug. 2015.

[11] X. Yu, Y. Fu, P. Li, and Y. Zhang, "Fault-tolerant aircraft control based on self-constructing fuzzy neural networks and multivariable SMC under actuator faults," *IEEE Trans. Fuzzy Syst.*, vol. 26, no. 4, pp. 2324–2335, Aug. 2018.

[12] H. Boubertakh and S. Labiod, "Optimal fuzzy PD controllers tuning using ACO for the stabilization of a quadrotor," *Neurosci. Lett.*, vol. 561, no. 1, pp. 203–207, 2015.

[13] C. Yin, Y. Chen, and S.-M. Zhong, "Fractional-order sliding mode based extremum seeking control of a class of nonlinear systems," *Automatica*, vol. 50, no. 12, pp. 3173–3181, Dec. 2014.

[14] X. Shi, Y. Cheng, C. Yin, S. Dadras, and X. Huang, "Design of fractional-order backstepping sliding mode control for quadrotor UAV," *Asian J. Control*, vol. 21, no. 1, pp. 156–171, Jan. 2019.

[15] S. Suzuki, T. Ishii, Y. Aida, Y. Fujisawa, K. Iizuka, and T. Kawamura, "Collision-free guidance control of small unmanned helicopter using nonlinear model predictive control," *SICE J. Control, Meas., Syst. Integr.*, vol. 7, no. 6, pp. 347–355, 2014.

[16] C.-T. Lee and C.-C. Tsai, "Nonlinear adaptive aggressive control using recurrent neural networks for a small scale helicopter," *Mechatronics*, vol. 20, no. 4, pp. 474–484, Jun. 2010.

[17] X. Shi, Y. Cheng, C. Yin, X. Huang, and S.-M. Zhong, "Design of adaptive backstepping dynamic surface control method with RBF neural network for uncertain nonlinear system," *Neurocomputing*, vol. 330, pp. 490–503, Feb. 2019.

[18] K. Dalamagkidis, K. P. Valavanis, and L. A. Piegl, "Nonlinear model predictive control with neural network optimization for autonomous autorotation of small unmanned helicopters," *IEEE Trans. Control Syst. Technol.*, vol. 19, no. 4, pp. 818–831, Jul. 2011.

[19] C. Yin, X. Huang, S. Dadras, Y. Cheng, J. Cao, H. Malek, and J. Mei, "Design of optimal lighting control strategy based on multi-variable fractional-order extremum seeking method," *Inf. Sci.*, vol. 465, pp. 38–60, Oct. 2018.

[20] H. Liang, L. Zhang, Y. Sun, and T. Huang, "Containment control of semi-Markovian multiagent systems with switching topologies," *IEEE Trans. Syst., Man, Cybern., Syst.*, early access, Oct. 28, 2019, doi: 10.1109/TSMC.2019.2946248.

[21] Q. Zhou, W. Wang, H. Liang, M. Basin, and B. Wang, "Observer-based event-triggered fuzzy adaptive bipartite containment control of multi-agent systems with input quantization," *IEEE Trans. Fuzzy Syst.*, early access, Nov. 15, 2019, doi: 10.1109/TFUZZ.2019.2953573.

[22] L. Wu and D. W. C. Ho, "Sliding mode control of singular stochastic hybrid systems," *Automatica*, vol. 46, no. 4, pp. 779–783, Apr. 2010.

[23] J. Knight, S. Shirsavar, and W. Holderbaum, "An improved reliability cuk based solar inverter with sliding mode control," *IEEE Trans. Power Electron.*, vol. 21, no. 4, pp. 1107–1115, Jul. 2006.

[24] K. Mei and S. Ding, "Second-order sliding mode controller design subject to an upper-triangular structure," *IEEE Trans. Syst., Man, Cybern., Syst.*, early access, Nov. 5, 2018, doi: 10.1109/TSMC.2018.2875267.

[25] S. Ding, J. H. Park, and C.-C. Chen, "Second-order sliding mode controller design with output constraint," *Automatica*, vol. 112, Feb. 2020, Art. no. 108704.

[26] F. Chen, R. Jiang, C. Wen, and R. Su, "Self-repairing control of a helicopter with input time delay via adaptive global sliding mode control and quantum logic," *Inf. Sci.*, vol. 316, pp. 123–131, Sep. 2015.

[27] F. Duan, C. He, and W. Zhang, "Application of feedback linearization and continuous sliding mode control to a nonlinear helicopter model," *Jetp Lett.*, vol. 104, no. 6, pp. 392–397, 2016.

[28] F. Chen, R. Jiang, K. Zhang, B. Jiang, and G. Tao, "Robust backstepping sliding-mode control and observer-based fault estimation for a quadrotor UAV," *IEEE Trans. Ind. Electron.*, vol. 63, no. 8, pp. 5044–5056, Aug. 2016.

[29] C. Yin, X. Huang, Y. Chen, S. Dadras, S.-M. Zhong, and Y. Cheng, "Fractional-order exponential switching technique to enhance sliding mode control," *Appl. Math. Model.*, vol. 44, pp. 705–726, Apr. 2017.

[30] J. Wang, C. Shao, and Y.-Q. Chen, "Fractional order sliding mode control via disturbance observer for a class of fractional order systems with mismatched disturbance," *Mechatronics*, vol. 53, pp. 8–19, Aug. 2018.

[31] C. Yin, Y. Cheng, S.-M. Zhong, and Z. Bai, "Fractional-order switching type control law design for adaptive sliding mode technique of 3D fractional-order nonlinear systems," *Complexity*, vol. 21, no. 6, pp. 363–373, Jul. 2016.

[32] X. Fang, A. Wu, Y. Shang, and N. Dong, "Robust control of small-scale unmanned helicopter with matched and mismatched disturbances," *J. Franklin Inst.*, vol. 353, no. 18, pp. 4803–4820, Dec. 2016.

[33] G. Antonelli, E. Cataldi, F. Arrichiello, P. R. Giordano, S. Chiaverini, and A. Franchi, "Adaptive trajectory tracking for quadrotor MAVs in presence of parameter uncertainties and external disturbances," *IEEE Trans. Control Syst. Technol.*, vol. 26, no. 1, pp. 248–254, Jan. 2018.

[34] M. Kabiri, H. Atrianfar, and M. B. Menhaj, "Formation control of VTOL UAV vehicles under switching-directed interaction topologies with disturbance rejection," *Int. J. Control*, vol. 91, no. 1, pp. 33–44, 2016.

[35] A. Mellit, G. M. Tina, and S. A. Kalogirou, "Fault detection and diagnosis methods for photovoltaic systems: A review," *Renew. Sustain. Energy Rev.*, vol. 91, pp. 1–17, Aug. 2018.

[36] M. T. Amin, S. Imtiaz, and F. Khan, "Process system fault detection and diagnosis using a hybrid technique," *Chem. Eng. Sci.*, vol. 189, pp. 191–211, Nov. 2018.

[37] R. C. Avram, X. Zhang, and J. Muse, "Quadrotor actuator fault diagnosis and accommodation using nonlinear adaptive estimators," *IEEE Trans. Control Syst. Technol.*, vol. 25, no. 6, pp. 2219–2226, Nov. 2017.

[38] E. Khalastchi and M. Kalech, "A sensor-based approach for fault detection and diagnosis for robotic systems," *Auto. Robots*, vol. 42, pp. 1231–1248, Dec. 2017.

[39] H. Li, H. Gao, P. Shi, and X. Zhao, "Fault-tolerant control of Markovian jump stochastic systems via the augmented sliding mode observer approach," *Automatica*, vol. 50, no. 7, pp. 1825–1834, Jul. 2014.

[40] K. Geng and N. A. Chulin, "Applications of multi-height sensors data fusion and fault-tolerant Kalman filter in integrated navigation system of UAV," *Procedia Comput. Sci.*, vol. 103, pp. 231–238, 2017.

[41] R. Zhang, J. Qiao, T. Li, and L. Guo, "Robust fault-tolerant control for flexible spacecraft against partial actuator failures," *Nonlinear Dyn.*, vol. 76, no. 3, pp. 1753–1760, May 2014.

[42] Z. Ding and Y. Shen, "Projective synchronization of nonidentical fractional-order neural networks based on sliding mode controller," *Neural Netw.*, vol. 76, pp. 97–105, Apr. 2016.

[43] C. Izaguirre-Espinosa, A. J. Muñoz-Vázquez, A. Sanchez-Orta, "Attitude control of quadrotors based on fractional sliding modes: Theory and experiments," *IET Control Appl.*, vol. 10, no. 7, pp. 825–832, 2016.

[44] C. Yin, S. Dadras, Y. H. Cheng, X. Huang, J. Cao, and H. Malek, "Multidimensional fractional-order Newton-based extremum seeking for online light-energy saving technique of lighting system," *IEEE Trans. Ind. Electron.*, early access, Nov. 6, 2019, doi: 10.1109/TIE.2019.2950867.

[45] S. Pashaei and M. Badamchizadeh, "A new fractional-order sliding mode controller via a nonlinear disturbance observer for a class of dynamical systems with mismatched disturbances," *ISA Trans.*, vol. 63, pp. 39–48, Jul. 2016.

[46] N. Ullah, W. Shaoping, M. I. Khattak, and M. Shafi, "Fractional order adaptive fuzzy sliding mode controller for a position servo system subjected to aerodynamic loading and nonlinearities," *Aerosp. Sci. Technol.*, vol. 43, pp. 381–387, Jun. 2015.

[47] M. Labbadi and M. Cherkaoui, "Robust adaptive backstepping fast terminal sliding mode controller for uncertain quadrotor UAV," *Aerosp. Sci. Technol.*, vol. 93, Oct. 2019, Art. no. 105306.

[48] O. Mofid and S. Mobayen, "Adaptive sliding mode control for finite-time stability of quad-rotor UAVs with parametric uncertainties," *ISA Trans.*, vol. 72, pp. 1–4, Jan. 2018.
[49] A. Aboudonia, A. El-Badawy, and R. Rashad, "Active anti-disturbance control of a quadrotor unmanned aerial vehicle using the command-filtering backstepping approach," *Nonlinear Dyn.*, vol. 90, no. 1, pp. 581–597, 2017.

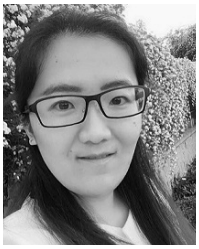

XIAOYU SHI was born in Shandong, China, in February 1992. She received the bachelor's degree in measurement and control technology and instrumentation from Xihua University, Chengdu, China, in 2015. She is currently pursuing the Ph.D. degree in instrument science and technology with the University of Electronic Science and Technology of China. Her research interests include robust control, unmanned aerial vehicle, sliding mode control, backstepping control, and control of under-actuated systems.

YUHUA CHENG (Senior Member, IEEE) received the Ph.D. degree from Sichuan University, Chengdu, China, in 2007. He has been a Professor with the School of Automation Engineering, University of Electronic Science and Technology of China, since 2015. His research interests include structural health monitoring, non-destructive testing and evaluation, and data acquisition.

CHUN YIN (Member, IEEE) received the Ph.D. degree from the University of Electronic Science and Technology of China, in 2014.

She was an exchange Ph.D. student with Utah State University, Logan, UT, USA, from 2011 to 2012, and the MESA Laboratory, University of California at Merced, CA, USA, from 2012 to 2013. She was an Associate Professor with the University of Electronic Science and Technology of China, from 2014 to 2019, where she has been a Professor with the School of Automation Engineering, since 2019. Her research interests include multi-objective evolutionary optimization, infrared thermography testing, and hypervelocity impact engineering. She won the Best New Scholars Award of the University of Electronic Science and Technology of China.

SHOUMING ZHONG was born in November 1955. He received the degree from the University of Electronic Science and Technology of China, majoring in applied mathematics on differential equation. He has been a Professor with the School of Mathematical Sciences, University of Electronic Science and Technology of China, since June 1997. His research interests include stability theorem and its application research of the differential systems, the robustness control, neural networks, and biomathematics. He is also the Director of the Chinese Mathematical Biology Society and the Chair of bio mathematics in Sichuan. He is also an Editor of the *Journal of Biomathematics*.

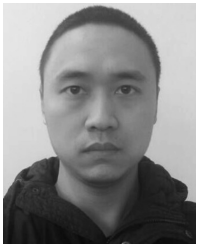

XUEGANG HUANG was born in November 1985. He received the B.S. degree from Southwest Jiaotong University, majoring in materials science and engineering, and the M.S. and Ph.D. degrees from the Mechanical Engineering College, Shijiazhuang, China, in 2010 and 2014, respectively. He is currently working with the Center of Aerodynamic Research and Develop of China, Hypervelocity Aerodynamic Institute. His research interests include advanced ceramic composites, space shielding engineering, hypervelocity impact engineering, and material dynamic behavior.

KAI CHEN received the Ph.D. degree from the University of Electronic Science and Technology of China, Chengdu, China, in 2015. He has been an Associate Professor with the School of Automation Engineering, University of Electronic Science and Technology of China, since 2017. His research interests include structural health monitoring and data acquisition.

GEN QIU received the B.S. and master's degrees from the University of Electronic Science and Technology of China, in 2005 and 2009, respectively. He is currently a Senior Engineer with the School of Automation Engineering, University of Electronic Science and Technology of China. His research interests include testing and measurement instrument design, and system reliability analysis and lifetime prediction technology.